A model of buoyant gas plume migration

Dmitriy Silin *

Lawrence Berkeley National Laboratory, 1 Cyclotron Road, MS 90-1116, Berkeley, CA 94720, USA

Tad W. Patzek

University of California, Berkeley, 425 Davis Hall, Berkeley, CA 94720, USA

Sally M. Benson

Energy Resources Engineering Department, Stanford University, 074 Green Sciences Building, 367 Panama Street, Stanford, CA 94305-22020, USA

Abstract

This work is motivated by the growing interest in injecting carbon dioxide into deep geological formations as a means of avoiding its atmospheric emissions and consequent global warming. Ideally, the injected greenhouse gases stay in the injection zone for a geologically long time and eventually dissolve in the formation brine and remain trapped by mineralization. However, one of the potential problems associated with the geologic method of sequestration is that naturally present or inadvertently created conduits in the cap rock may result in a gas leakage from primary storage. Even in supercritical state, the carbon dioxide viscosity and density are lower than those of the formation brine. Buoyancy will tend to drive the leaked CO_2 plume upward. Theoretical and experimental studies of buoyancy-driven supercritical CO_2 flow, including estimation of time scales associated with plume evolution and migration, are critical for developing technology, monitoring policy, and regulations for safe carbon dioxide geologic sequestration.

In this study, we obtain simple estimates of vertical plume propagation velocity taking into account the density and viscosity contrast between CO_2 and brine. We describe buoyancy-driven countercurrent flow of two immiscible phases by a Buckley-Leverett type model. The model predicts that a plume of supercritical carbon dioxide in a homogeneous water-saturated porous medium does not migrate upward like a bubble in bulk water. Rather, it spreads upward until it reaches a seal or until the fluids become immobile. A simple formula requiring no complex numerical calculations describes the velocity of plume propagation. This solution is a simplification of a more comprehensive theory of countercurrent plume migration (Silin et al., 2007). In a layered reservoir, the simplified solution predicts a slower plume front propagation relative to a homogeneous formation with the same harmonic mean permeability. On the contrary, the model yields much higher plume propagation estimates in a high-permeability conduit like a vertical fracture.

Key words: geologic sequestration, buoyancy, countercurrent flow, plume migration

1 Introduction

This work is motivated by the growing interest in injecting carbon dioxide into deep geological formations as a means of avoiding its atmospheric emissions

* Corresponding author.
Email addresses: DSilin@lbl.gov (Dmitriy Silin), patzek@parzek.berkeley.edu (Tad W. Patzek), SMBenson@stanford.edu (Sally M. Benson).

and consequent global warming. Ideally, the injected gas stays in the injection zone for a long time and will be dissolved in the formation brine and trapped by mineralization. However, a gas leakage from primary storage may occur because of cracks or other naturally or inadvertently man-made conduits in the cap rock. Even if the injected carbon dioxide is in supercritical state, its viscosity and density are lower than those of the indigenous formation brine. Therefore, buoyancy always drives the injected carbon dioxide upward. Understanding the buoyancy-driven plume migration and estimation of the time scales associated with plume evolution are critical for developing appropriate regulations providing for the safety of potable water resources.

The objective of this study is to characterize the evolution of a plume of supercritical carbon dioxide in water-saturated porous medium. We estimate the velocity of plume propagation taking into account the density and viscosity contrast between the injected CO_2 and formation water. This work follows previous studies (Silin et al., 2006, 2007) where a more general model of two-phase vertical countercurrent flow has been discussed. Here, we simplify that model by neglecting capillary forces. This simplification leads to a more transparent theory while preserving the main conclusion of the more general approach. Two-phase flow is characterized by a hyperbolic equation, which is then solved using method of characteristics (Petrovskii, 1966; Lax, 1973). Mathematically, the evolution of the plume is described as a sequence of exact solutions usually called shock and rarefaction waves. The theory predicts that in a porous medium, the plume does not migrate upward like a gas bubble in bulk water. Rather, the gas spreads upward until it hits a seal or reaches a uniform immobile gas saturation. The simplified model discussed here predicts the same plume propagation velocity estimates as the model studied by Silin et al. (2007).

The hyperbolic flow model can be easily extended to heterogeneous media. In particular, we consider propagation of the front of the plume through a layered aquifer. The theory predicts that a low-permeability layer significantly reduces the speed of propagation in all overlaying strata. Simulations of plume propagation in a laterally heterogeneous formation predict dispersion of the front of the plume. If the heterogeneity of the medium includes a conductive vertical fracture, then propagation of the plume inside the fracture is much faster than in the rest of the formation.

We believe that the theory developed here provides reasonable estimates of the time of plume propagation from the formation flow properties. Field and experimental work will help to scale and calibrate the most important parameters.

Section 2 briefly overviews extension of Buckley–Leverett hyperbolic model to buoyancy-driven two-phase countercurrent flow. Section 3 discusses typical solutions and their physical interpretations, both for homogeneous and heterogeneous formations. Conclusions and recommendations are summarized in sections 4 and 5. For brevity, the injected supercritical carbon dioxide will be called gas.

2 The model

A carbon dioxide plume migration involves various complex processes acting in different time scales. Juanes et al. (2006) formulate five principal mechanisms of CO_2 trapping: hydrodynamic trapping, solution trapping, mineral trapping, capillary trapping, and two-phase flow hysteresis. The latter is a consequence of gas trapping by water imbibing in water-wet rocks (Al-Futaisi and Patzek, 2003; Valvante and Blunt, 2004).

In this work, we focus on buoyancy-driven two-phase viscous flow. This choice is based on the assumption that other processes, like dissolution and geochemistry, are much slower than the flow. In addition, if a leaking plume loses carbon dioxide at a certain rate as it migrates under buoyancy, such losses can only slow down the plume propagation, Thus, the estimates obtained here can be qualified as the worst-case scenario.

2.1 Buckley–Leverett model of two-phase flow

Assume that the carbon dioxide plume crosses a thick aquifer with uniform flow properties. Let the vertical coordinate, z, be directed upward. Thus, a positive Darcy velocity means upward flow. Darcy's law for two-phase flow states the following relationships between the Darcy velocities of gas and brine and their respective pressure gradients (Muskat, 1949; Hubbert, 1956):

$$u_g = -\frac{k_{rg}(S)k}{\mu_g}\left(\frac{\partial p_g}{\partial z} - \varrho_g g\right) \tag{1}$$

$$u_w = -\frac{k_{rw}(S)k}{\mu_w}\left(\frac{\partial p_w}{\partial z} - \varrho_w g\right) \tag{2}$$

Here u_g and u_w are Darcy velocities, or volumetric fluxes, of the gas and liquid, μ_g and μ_w are the dynamic viscosities of the fluids, p_g and p_w, and ϱ_g and ϱ_w are their pressures and densities, respectively. The brine volumetric saturation and gravity acceleration are denoted by S and g, and k is the absolute permeability of the medium. In this derivation, we neglect the compressibility of brine and supercritical gas. Since there is no sink or source of gas or brine, the flow is countercurrent:

$$u_g + u_w = 0 \tag{3}$$

To obtain equations in dimensionless form, we introduce dimensionless vertical coordinate ζ and time τ:

$$\zeta = \frac{z}{H} \qquad \tau = \frac{k\,(\varrho_w - \varrho_g)\,g}{\mu_w H}\,t \tag{4}$$

Here H is the thickness of the reservoir. In what follows, we assume that the following condition holds true:

$$\left|\gamma \mathcal{J}'(S)\frac{\partial S}{\partial \zeta}\right| \ll 1 \tag{5}$$

where

$$\gamma = \frac{\sigma}{(\varrho_w - \varrho_g)gH}\sqrt{\frac{\phi}{k}} \tag{6}$$

is an analog of the reciprocal Bond number. Under assumption (5), the impact of capillarity is negligible (Silin et al., 2006).

Combination of Darcy's law with mass the balance yields a hyperbolic equation for brine saturation S:

$$\phi\frac{\partial S}{\partial \tau} - \frac{\partial}{\partial \zeta} f(S) = 0 \tag{7}$$

where

$$f(S) = \frac{k_{rw}(S)}{\dfrac{k_{rw}(S)}{k_{rg}(S)}\dfrac{\mu_g}{\mu_w} + 1} \tag{8}$$

Equation (7) constitutes a Buckley–Leverett type flow model (Buckley and Leverett, 1942) in dimensionless form. The dimensionless Darcy velocity of brine

$$W_w = \frac{\mu_w}{k(\varrho_w - \varrho_g)g} u_w \tag{9}$$

equals minus partial flow function:

$$W_w = -f(S) \tag{10}$$

2.2 *Shock and rarefaction wave solutions*

A solution to a hyperbolic equation like Equation (7) propagates along characteristics (Petrovskii, 1966; Lax, 1973). The theory predicts two types of stable saturation profiles. Using the terminology of gas dynamics (Landau and Lifshitz, 1959), such profiles are called shock and rarefaction waves. In the model under consideration, a solution of the first type characterizes an abrupt variation of the saturation profile. The second one characterizes a stretching smooth saturation profile.

Consider a shock wave. If S_1 and S_2 denote the saturations ahead and behind the front, then mass conservation yields the following expression for the dimensionless shock propagation velocity:

$$V_s(S_1, S_2) = -\frac{1}{\phi}\frac{f(S_2) - f(S_1)}{S_2 - S_1} \tag{11}$$

Note that the expression on the right-hand side can be either positive or negative, or can be equal to zero for an equilibrium saturation transition.

A rarefaction-wave saturation profile is provided by the implicit relationship

$$\zeta = \zeta_0 - \tau\frac{1}{\phi}f'\left(S(\tau, \zeta)\right) \tag{12}$$

where ζ_0 is the initial location of the center of the wave. Equation

$$V_r(S) = -\frac{1}{\phi}f'\left(S\right) \tag{13}$$

expresses the velocity of propagation of the part of the rarefaction wave, where the brine saturation is equal to S. If a shock wave with saturations S_1 and S_2 before and behind the front is followed or preceded by a rarefaction wave, then the conservation of mass implies

$$f'(S_i) = \frac{f(S_2) - f(S_1)}{S_2 - S_1} \tag{14}$$

where i is either 1 or 2.

3 Results and Discussion

We begin with describing evolution of the plume in a homogeneous formation as a sequence of shock and rarefaction waves. The theory of two-phase buoyancy-driven flow predicts that the main part of the plume practically stays put, being reduced from the top part by the leading propagating front. Evolution of this leading front is much faster that the evolution of the rest of the plume. The leading is relatively lean with respect to gas saturation. For simplicity, we consider an initial plume with a constant gas saturation. We put the origin $z = 0$ at the top of the initial plume (Figure 1).

3.1 The leading front of the plume

In estimating the plume propagation time, the most critical part is the top leading front of the plume. Assuming that the formation ahead of the plume is entirely saturated by water, Equations (4) and (11) imply that the dimensionless front propagation velocity is equal

$$V^* = \frac{1}{\phi} \frac{f(S^*)}{1 - S^*} \tag{15}$$

In physical units,

$$v^* = \frac{k(\varrho_w - \varrho_g)g}{\phi \mu_w} \frac{f(S^*)}{1 - S^*} \tag{16}$$

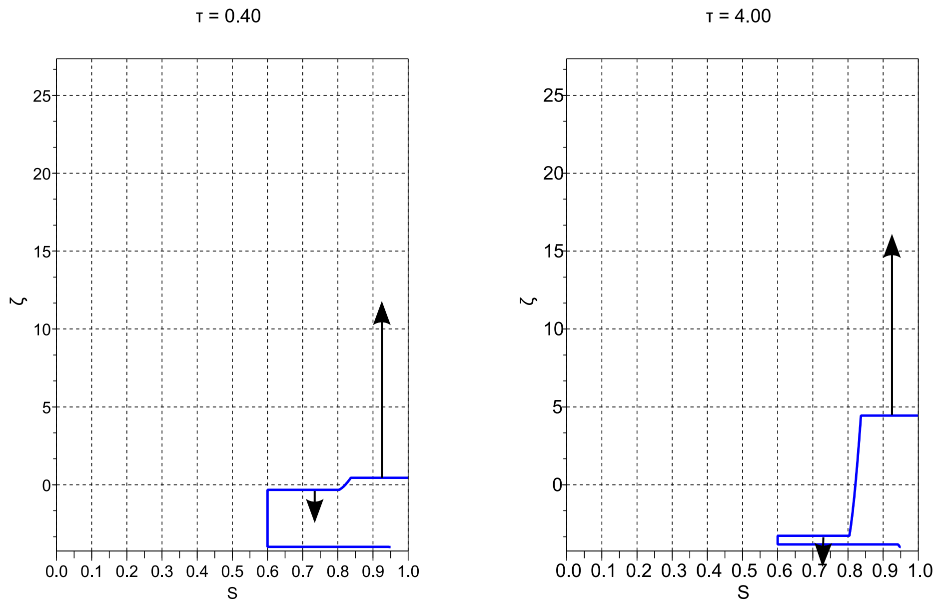

Fig. 1. Vertical brine saturation profile at an early stage of plume evolution. The initial saturation of gas is 40 %. A leading front of low gas saturation propagates upward, whereas the main part of the plume gradually shrinks. The arrows show the directions of propagation of the fronts.

3.2 Evolution of the main part of the plume

The evolution of the saturation profile behind the leading part of the plume described in the previous subsection can be characterized as a sequence of two rarefaction and two shock waves. Figures 1–3 display the profiles at different times in dimensionless units. The theory predicts three stages of plume evolution. At early time, the high-gas-saturation part of the plume thins between two traveling shock waves in the saturation profile propagating in the opposite directions (Figure 1). At the top, a travelling wave propagates downward to compensate for the flow of gas in the leading part. At the bottom of the plume, the shock in the saturation profile propagates upward. This shock-wave solution is proceeded by a rarefaction wave. The evolution of the bottom part

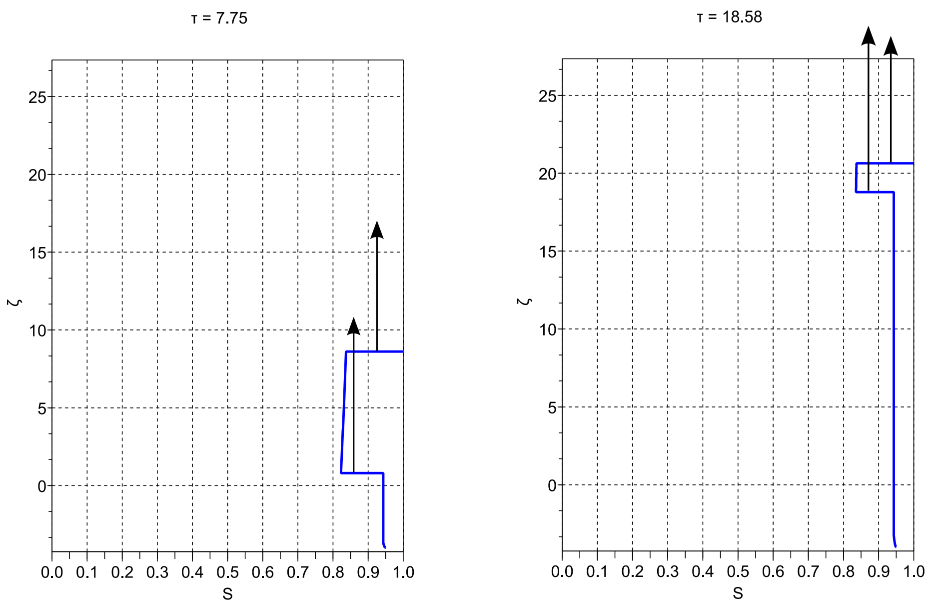

Fig. 2. Evolution of the plume after its main part collapses. The lean leading part of the plume migrates upward whereas gas saturation behind it approaches the residual saturation.

of the plume is extremely slow at early times and is barely noticeable in the plots. Due to roundoff errors, numerical simulations may entirely miss it along with the following traveling wave (Riaz and Tchelepi, 2006). The slowness is a consequence of the water-wet environment where the permeability to water drops dramatically in the presence of gas. The high (relative to the gas) water viscosity further slows down fluid exchange.

When the main part of the plume collapses, the evolution of the bottom part of the saturation profile becomes faster, see Figure 2. Since the leading part of the saturation profile keeps on propagating with the same velocity, the traveling wave at the bottom compensates for the gas flow by propagating upward. Note that the speed of propagation of the bottom traveling wave exceeds V^*, given by Equation (15). Another interesting feature of this phase of plume evolution is that the saturation at the junction between the bottom rarefaction wave

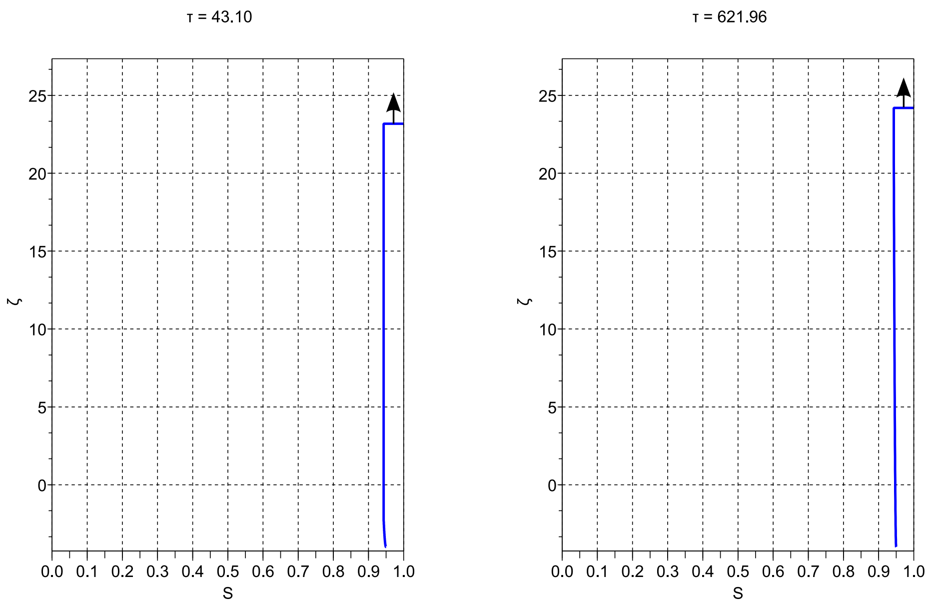

Fig. 3. The final phase of plume evolution. The bottom rarefaction wave characterizes the saturation profile in most of the plume. The gas is closed to being trapped over the entire plume.

and the rarefaction wave of the leading part of the plume, S_R, becomes a function of time, $S_R = S_R(\tau)$. Hence, the velocity of propagation evaluated from Equation (11) also becomes a function of time. However, calculations (omitted in the present work) show that the variation of this velocity is small.

This plume configuration remains viable until the part of the saturation bounded by the top and bottom traveling shock waves collapses. Once this happens, the saturation along the entire plume is close to the residual gas saturation. The plume continues to thin through the rarefaction wave centered at the bottom, Figure 3. Since the saturation of water in this last stage exceeds S^* in the entire plume, the propagation of the top of the plume slows down dramatically. The theory suggests asymptotic convergence of the saturation profile to the residual gas saturation.

3.3 *Evolution of a plume at a horizontal interface*

The theory developed above is for an idealized homogeneous formation. In this section, we consider propagation of the leading top of the plume through a horizontal interface between two different rocks. The subscript index $_1$ will denote the formation below the interface, and the index $_2$ will denote the formation above the interface. Thus, let ϕ_1 and k_1 characterize the porosity and permeability of the rock underneath the interface, and ϕ_2 and k_2 characterize the porosity and permeability of the rock above the interface. Let S_1 be the saturation at the leading front on the top of the plume before crossing the interface. The gas Darcy velocity at this saturation is given by

$$u_1 = \frac{k_1(\varrho_w - \varrho_g)g}{\phi_1 \mu_w} f_1(S_1) \tag{17}$$

On both sides of the interface, Darcy velocity of gas must be the same:

$$\frac{k_1(\varrho_w - \varrho_g)g}{\phi_1 \mu_w} f_1(S_1) = \frac{k_2(\varrho_w - \varrho_g)g}{\phi_2 \mu_w} f_2(S_2) \tag{18}$$

The fluid densities and viscosities cancel, so the last equation relates water saturations on both sides of the interface to the variation of rock properties.

Let a superscript asterisk * denote the saturation corresponding to the maximum velocity of propagation of the top front of the plume, and a superscript ^{M} denote the maximum of the partial flow function:

$$\frac{f_i(S_i^*)}{1 - S_i^*} = \max_S \frac{f_i(S)}{1 - S}, \quad f_i(S_i^M) = \max_S f_i(S), \quad i = 1, 2 \tag{19}$$

In mass balance equation (18), S_1 is the saturation at the top of propagating plume. In a homogeneous medium, $S_1 = S_1^*$. It may be not the case if a plume crosses in interface.

First, let us consider a case where there is no S_2 satisfying mass balance equation (18). This happens when the permeability of Medium 2 is insufficient to support gas flow in Medium 1. Therefore, gas saturation will start growing at the interface and the flow rate will slow down correspondingly. The brine saturation in Medium 1 at the boundary will reach some value S_1', which is less or equal to S_1^*, so that the Darcy velocity in Medium 1 will match the maximum Darcy velocity in Medium 2:

$$\frac{k_1}{\phi_1} f_1(S_1') = \frac{k_2}{\phi_2} f_2(S_2^*) \tag{20}$$

Here, we have cancelled similar terms from Equation (18). We are interested in the smaller of the two saturations, S_1', satisfying Equation (20). Gas accumulation at the interface generates two shock waves on the saturation profile: an upward wave in Medium 2 with the velocity of propagation

$$v_2^* = \frac{k_2(\varrho_w - \varrho_g)g}{\phi_2 \mu_w} \frac{f_2(S_2^*)}{1 - S_2^*} \tag{21}$$

and a shock wave in Medium 1 with the velocity of propagation

$$v_1' = -\frac{k_1(\varrho_w - \varrho_g)g}{\phi_1 \mu_w} \frac{f_1(S_1^*) - f_1(S_1')}{S_1^* - S_1'} \tag{22}$$

Saturation S_1' is lesser than S_1^* due to gas accumulation. Since this gas accumulation reduces the Darcy velocity in order to equalize it with the fluid flow in Medium 2, one has $f_1(S_1') < f_1(S_1^*)$. The velocity v_1' is negative and the shock wave propagates downward, Figure 4.

Now, let the saturation S_1 be such that Equation (18) has a solution S_2. Then, unless $S_2 = S_2^*$, there are two different saturations satisfying Equation (18). Since the plume propagates into a fully brine-saturated formation, only the larger solution is physically sensible. If saturation S_2 obtained from Equation (18) does not exceed S_2^*, $S_2 \leq S_2^*$, then the gas supply from Medium 1 is

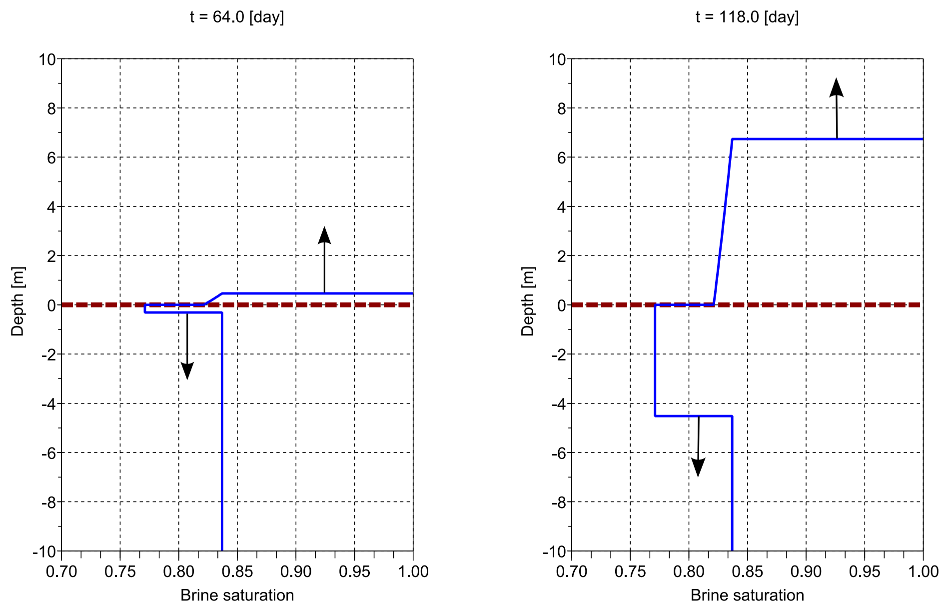

Fig. 4. A plume crossing the boundary: the permeability of the formation above the interface is less than that of the formation beneath the boundary (bold dashed line). Accumulation of gas beneath the boundary generates a shock wave traveling downward. The arrows show the directions of propagation of the fronts.

sufficient to support the maximum velocity of plume propagation in Medium 2. In such a case, the plume propagates into Medium 2 with the theoretically maximal velocity described by Equation (21). The leading shock wave is followed by a rarefaction wave. The latter may or may not extend all the way to the stable point of maximal Darcy velocity, that is to the saturation S_2^M, Figure 5.

If the arriving plume is so lean with respect to gas that the brine saturation S_2 obtained from the continuity equation (18) exceeds S_2^*, then the velocity of plume propagation in Medium 2 is

$$v_2 = \frac{k_2(\varrho_w - \varrho_g)g}{\phi_2 \mu_w} \frac{f_2(S_2)}{1 - S_2} < v_2^* \tag{23}$$

Figure 6 shows propagation of a lean plume.

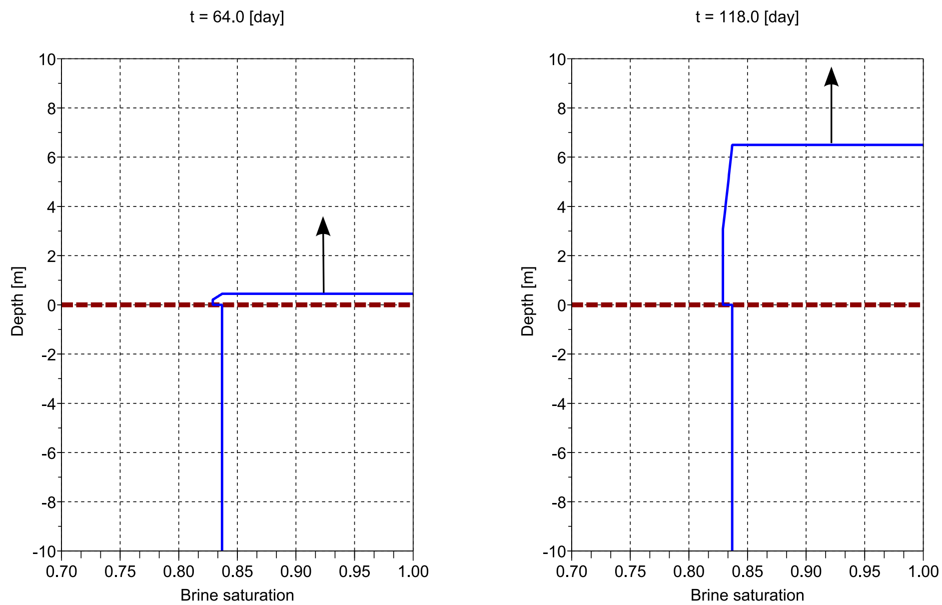

Fig. 5. A plume crossing the boundary: the formation permeability above the interface is slightly less than that beneath the boundary (bold dashed line). The rarefaction wave behind the leading front is incomplete.

3.4 Plume propagation in a heterogeneous formation

Let us consider a formation of thickness H subdivided into zones with different properties. Inside each zone, the formation is assumed homogeneous. Let N be the total number of zones and H_i be the thickness of layer i, numbered in the direction of the plume propagation: from the bottom to the top. To evaluate the time of the plume crossing each layer, one needs to estimate the respective velocity v_i of the plume propagation. We do such an estimate using the results of the previous subsection.

In each layer, the velocity of plume propagation is either equal to the theoretical maximum, v_i^*, or is less than that if the underlying low-permeability layers reduce the actual velocity to a lower value. In the first case, the time of

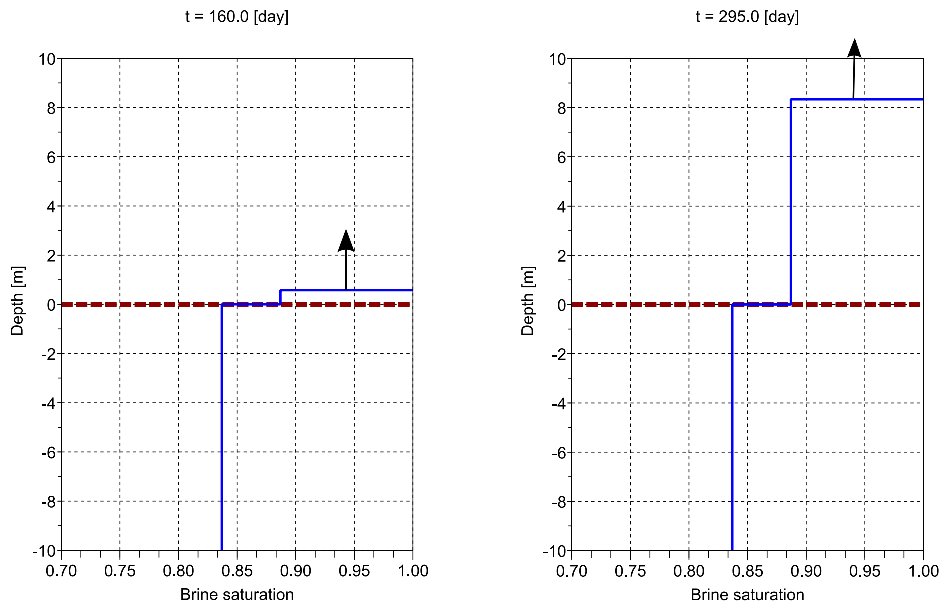

Fig. 6. Lean plume behind the boundary: the gas supply below the boundary (bold line) is insufficient to support the maximum velocity of propagation above the boundary. The time elapsed between the shown saturation profiles is one month. The arrows show the direction of propagation of the front.

crossing the layer can be estimated upfront:

$$\tau_i^* = \frac{H_i}{v_i^*} = \frac{\phi_i \mu_w H_i}{k_i(\varrho_w - \varrho_g)g} \frac{1 - S_i^*}{f_i(S_i^*)} \tag{24}$$

If the maximal velocity of propagation is possible in all sublayers, then the total time, T^*, is determined by summation

$$T^* = \sum_i \frac{\phi_i \mu_w H_i}{k_i(\varrho_w - \varrho_g)g} \frac{1 - S_i^*}{f_i(S_i^*)} \tag{25}$$

This is the theoretical minimum of plume propagation time.

Now, let us consider a case where the maximal velocity of propagation is unfeasible in all layers. In such a case, the saturations at the top front of the plume must be calculated by a sequential solution of equation (18) from the bottom layer to the top. In particular,

$$f_i(S_i) = \frac{k_i \phi_{i-1}}{k_{i-1}\phi_i} f_{i-1}(S_{i-1}) \tag{26}$$

The time of crossing of the layer i is equal to

$$\tau_i = \frac{\phi_i \mu_w H_i}{k_i(\varrho_w - \varrho_g)g} \frac{1 - S_i}{f_i(S_i)} \tag{27}$$

Repeatedly applying equation (26), one gets

$$f_i(S_i) = \frac{k_i}{\phi_i} \frac{\phi_1}{k_1} f_1(S_1) \tag{28}$$

After substitution of this result into Equation (27) and summation in i, the total travel time is

$$T = \frac{\mu_w}{(\varrho_w - \varrho_g)g} \frac{\phi_1}{k_1} \frac{1}{f_1(S_1)} (1 - \overline{S})H \tag{29}$$

where $\overline{S}$ is the mean brine saturation:

$$\overline{S} = \sum_i S_i \frac{H_i}{H} \tag{30}$$

Equation (29) relates the mean velocity of propagation of the plume in a heterogeneous formation, $\overline{v}$, to the mean brine saturation

$$\overline{v} = \frac{k_1(\varrho_w - \varrho_g)g}{\phi_1 \mu_w} \frac{f_1(S_1)}{1 - \overline{S}} \tag{31}$$

If the permeability and porosity distributions $k(z)$ and $\phi(z)$ are known, and the dimensionless fractional flow function does not depend on depth, then, in case of a non-maximal plume propagation velocity, the saturation distribution can be predicted from Equation (28):

$$S(z) = f^{-1}\left(\frac{k(z)}{\phi(z)} \frac{\phi_1}{k_1} f_1(S_1)\right) \tag{32}$$

This equation leads to an estimate of the mean saturation at the leading front of the plume and, respectively, to an estimate of the plume travel time.

3.5 The impact of heterogeneity on plume propagation time

Let us assume that the relative permeability curves are the same for the rock above and below the interface, so that one can use the same fractional flow function, $f(S)$. Then, water saturation at the leading front of the plume is always equal or exceeds S^*. Calculations in the previous section suggest the following rule of estimating the velocity of propagation when the plume crosses an interface between two media. If

$$f(S^*) \leq \frac{k_1 \phi_2}{k_2 \phi_1} f(S_1) \tag{33}$$

then $S_2 = S^*$ and the plume propagation speed in Medium 2 is at maximum. If the opposite inequality holds true, then S_2 must be determined from Equation (20), and Equation (23) determines the velocity of plume propagation. This calculation must be repeated for all layers from the bottom to the top.

For illustration, consider a layered formation with a random permeability distribution, see Figure 7. Figure 8 shows plume propagation as a function of time, accounting for the variations in permeability and ignoring it by using the harmonic mean permeability of all layers as an effective uniform permeability. This example shows that heterogeneous layers slow down plume propagation. The nature of this phenomenon is in the nonlinear dependence of the flow on fluid saturation. As a consequence, the saturation in a high-permeability layer overlaying a low-permeability layer can be different from the saturation S^*.

To quantify the impact of heterogeneity on the time of plume propagation, a

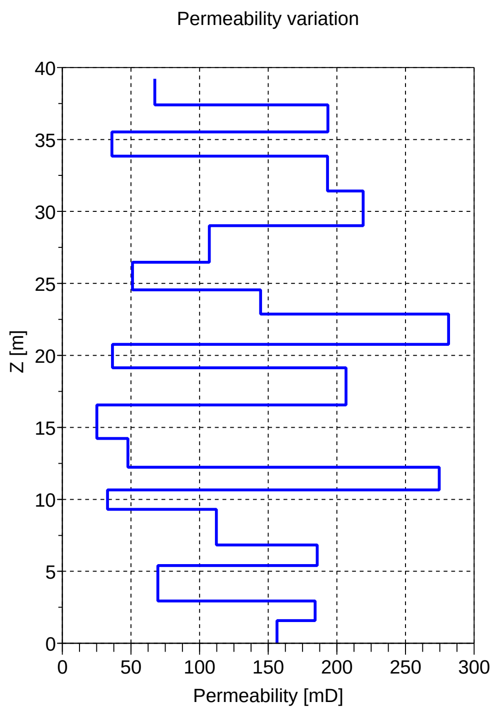

Fig. 7. Vertical permeability profile.

number of simulations has been run for various realizations of random distribution of the absolute permeability. The aquifer in this example consists of 20 equally-thick layers of different permeabilities. Each layer is 2-meters thick. The standard deviation of the permeability scaled by the harmonic mean quantifies the heterogeneity of the formation. Similar to example in Figure 8, two propagation times are evaluated for each realization. Fist, the propagation time is evaluated accounting for the heterogeneities as described earlier in this section. Second, the propagation time is predicted under the assumption that the entire aquifer is homogeneous and the effective permeability equals the harmonic mean of the layer permeabilities. The measure of delay is the ratio of the two times, which is a dimensionless quantity. Figure 3.5 shows the results obtained for 250 realizations. It shows a linear trend (solid line) of increasing time delay with increasing heterogeneity.

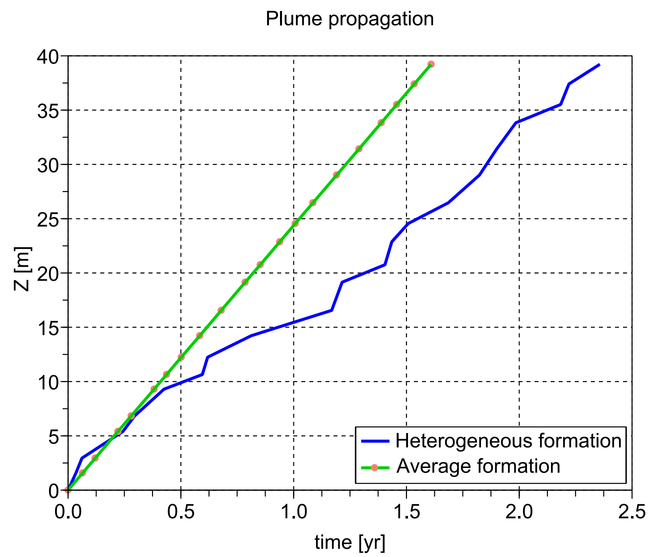

Fig. 8. Vertical plume propagation versus time. The straight line shows propagation in a homogeneous formation with the harmonic mean of permeability from the profile in Figure 7. The polygonal line has been calculated accounting for the heterogeneity. The dots are centered at the boundaries between the layers.

3.6 Front dispersion in a laterally heterogeneous medium

In this section we evaluate the impact of lateral heterogeneity on dispersion of the front of the plume. For this purpose, we consider a vertical cross-section of an aquifer with the dimensions and distribution of permeability shown in Figure 10. In this computer-generated medium, we apply the model of vertical flow developed above. The simulations involve a percolation-like algorithm with account for the time of plume evolution. Our model neglects lateral flow, so the estimates and calculations are just a first approximation. However, due to the analytical nature, these calculation are practically free of discretization

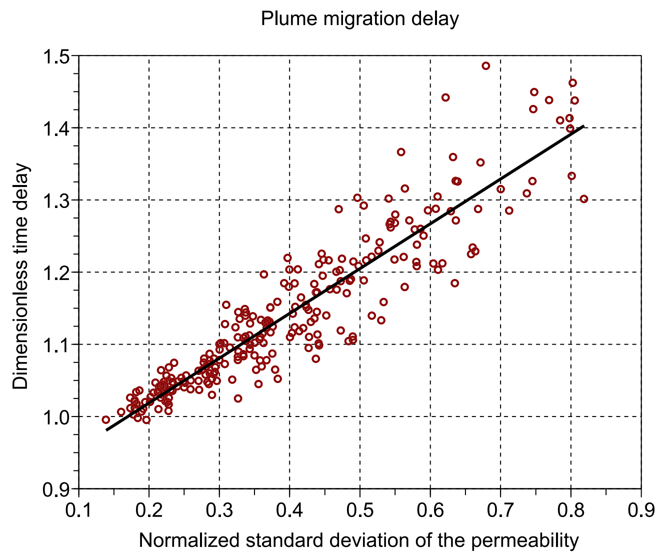

Fig. 9. Dimensionless plume delay versus normalized variance of permeability.

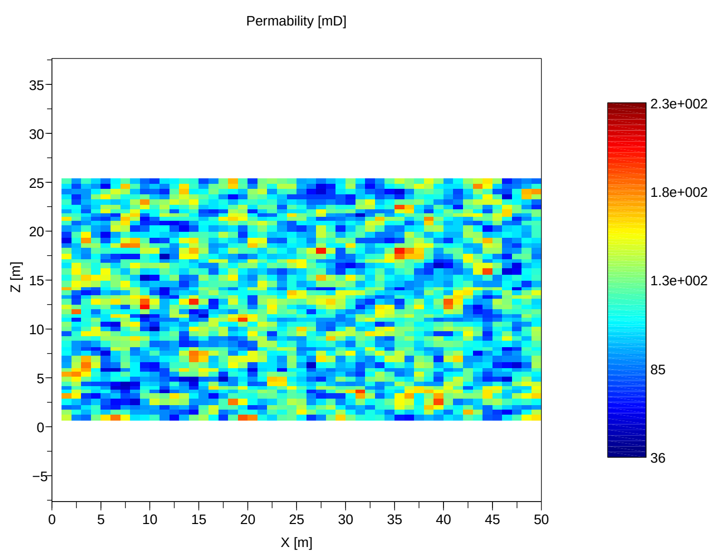

Fig. 10. A computer-generated vertical cross-section of heterogeneous formation.

errors. Figure 11 shows the dispersion of the front of the plume caused by the heterogeneity.

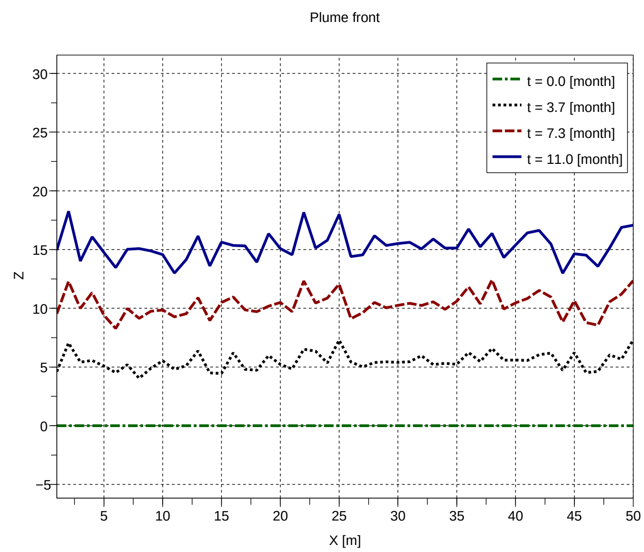

Fig. 11. Front propagation in formation shown in Figure 10.

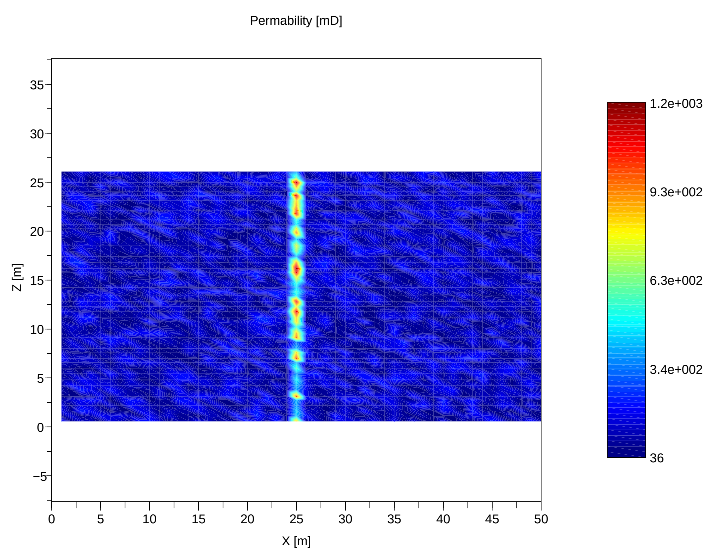

Fig. 12. A computer-generated vertical cross-section of heterogeneous formation with a permeable crack in the center.

The result is significantly different if there is a permeable vertical conduit, like a crack, Figure 12. Figure 13 shows fast propagation of the plume inside the crack, whereas the character of front propagation in the rest of the plume is similar to that in Figure 11.

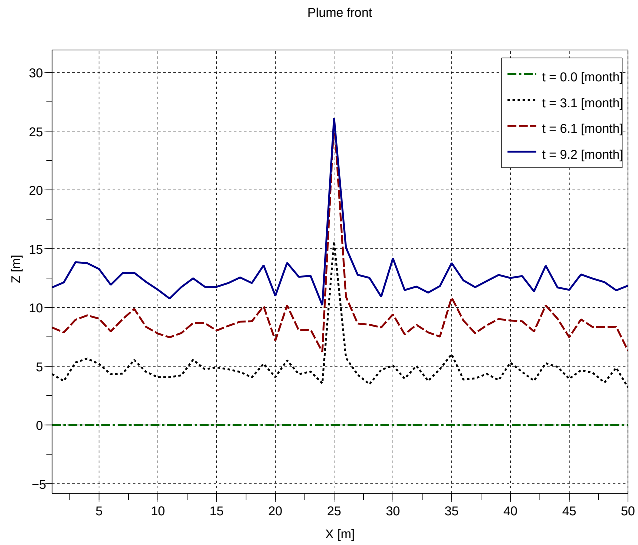

Fig. 13. Front propagation in a permeable vertical crack is much faster than in the rest of the plume.

4 Summary and conclusions

Buoyancy-driven viscous flow of a gas plume is modelled as one-dimensional two-phase countercurrent flow. This approximation is applicable to the flow far enough from the lateral boundaries of the plume. In a vertical fracture or other laterally confined brine-saturated structure the flow also can be described as one-dimensional. Under certain conditions, the capillary effects can be neglected, which leads to a hyperbolic model of flow. The method of characteristics suggests two types of solutions: shock and rarefaction waves. This approach predicts that in a porous medium, the gas plume does not migrate like a bubble in bulk water. Instead, the leading part of the plume, having relatively low gas saturation propagates much faster than the main part of the plume, which stays practically put. The saturation in the leading part of the plume can be estimated from the dimensionless fractional flow function through a simple calculation.

The theory admits an extension to a heterogeneous aquifer. For a simple model of layered formation, it suggests rules of plume flow across an interface between two adjacent layers with different rock properties. Iteration of this rule leads to a prediction of the evolution of gas plume in a layered reservoir. The principal conclusion is that a layered heterogeneity slows down propagation of the plume. Therefore, estimates based on a homogeneous medium with effective permeability can be wrong. The reason of the slowing-down impact of heterogeneity is that a single low-permeability layer dramatically reduces the plume propagation velocity in all overlaying strata. Therefore, an intact seal plays a critical role in the containment of injected CO_2 for a long time. Statistical analysis of evaluation of plume travel time delay due to heterogeneity leads to a linearly increasing trend of this delay relative the standard deviation of the permeability distribution between the layers.

A flow model involving lateral heterogeneity of the formation predicts dispersion of the front of the plume. In spite of the viscosity contrast between supercritical carbon dioxide and formation liquid, our model-based calculations have not indicated development of fingering at the front. Simulations show a completely different picture if the formation includes a highly-permeable vertical nonconformity, like a vertical crack. In such a case, even if the mean permeability of the crack is only slightly larger than that of the rest of the domain, plume propagation in the crack is much faster than in the other regions of the formation. The calculations do not account for lateral fluid flow component. At the same time, they are based on explicit formulae excluding any errors or numerical dispersion associated with discretization.

5 Recommendations

The character of the evolution of vertical saturation profile implied by the theory developed here suggests that in a homogeneous reservoir a laterally-distributed plume should spread over the overlaying formation. To maximize the volume of trapped gas, it seems attractive to inject it at the bottom part of an aquifer in such a way that the plume spreads laterally as much as possible. Apparently, such injection pattern can be achieved by creation of horizontal fractures at the bottom of injection interval. However, such a strategy may also increase risk of gas leakage if the plume reaches a fracture or a permeable fault.

Acknowledgments

This work was supported by the U.S. Department of Energy's Assistant Secretary for Coal through the Zero Emission Research and Technology Program under US Department of Energy contract no. DE-AC02-05CH11231 to Lawrence Berkeley National Laboratory (LBNL). The authors a grateful to Dr. Andrea Cortis and Dr. Stefan Finsterle of LBNL for reviewing the manuscript and suggesting numerous improvements.

References

Al-Futaisi, A., Patzek, T. W., 2003. Impact of wettability on two-phase flow characteristics of sedimentary rock: Quasi-static model. Water Resources Research 39 (2), 1042–1055.

Buckley, S. E., Leverett, M. C., 1942. Mechanisms of fluid displacement in sands. Trans. AIME 146, 149–158.

Hubbert, M. K., 1956. Darcy's law and the field equations of the flow of underground fluids. Trans. AIME 207 (7), 222–239.

Juanes, R., Spiteri, E. L., Orr Jr., F. M., Blunt, M. J., 2006. Impact of relative permeability hysteresis on geologic CO_2 storage. Water Resources Research 42, W12418, doi:10.1029/2005WR004806.

Landau, L. D., Lifshitz, E. M., 1959. Course of Theoretical Physics. Fluid Mechanics. Vol. 6 of Series in advanced physics. Addison-Wesley, Reading, Mass.

Lax, P., 1973. Hyperbolic Systems of Conservation Laws and the Mathematical Theory of Shock Waves. Society of Industrial and Applied Mathematics, Philadelphia.

Muskat, M., 1949. Physical Principles of Oil Production. McGraw-Hill, New York, NY.

Petrovskii, I. G., 1966. Ordinary differential equations. Prentice-Hall, Englewood Cliffs, NJ.

Riaz, A., Tchelepi, H. A., 2006. Dynamics of vertical displacement in porous media associated with CO_2 sequestration. SPE paper 103169. In: 2006 SPE Annual Technical Conference and Exhibition. September 24–27, 2006. SPE, San Antonio, TX.

Silin, D., Patzek, T. W., Benson, S. M., September 2006. Exact solutions in a model of vertical gas migration. SPE paper 103156. In: 2006 SPE Annual Technical Conference and Exhibition. September 24–27, 2006. SPE, San Antonio, TX.

Silin, D., Patzek, T. W., Benson, S. M., 2007. A model of buoyancy-driven two-phase countercurrent fluid flow. Laboratory report LBNL-62607, Lawrence

Berkeley National Laboratory, Berkeley, CA.

Valvante, P. H., Blunt, M. J., 2004. Predictive pore-scale modeling of two-phase flow in mixed-wet media. Water Resources Research 40, W07406, doi:10.1029/2003WR002627.